

# Simultaneous Measurements of Pressure and Deformation on a UCAV in the SARL

Jim Crafton\*, Sergey Fonov\*, E. Grant Jones\*, Vladimir Fonov\*, Larry Goss\*  
Innovative Scientific Solutions, Inc

Charles Tyler\*  
Air Force Research Lab

## Abstract

The assessment of advanced technology in the air force is becoming more reliant on the accuracy and fidelity of numerical predictions. It is expedient therefore, to validate the numerical codes upon which these assessments are based. The validation process requires the direct comparison of experimental measurements and numerical predictions. Among the issues that hinder the comparison of experimental measurements and computational predictions is the accuracy and structural integrity of the physical model. The ability to monitor the structural deformation of the model while simultaneously acquiring experimental data is of significant value. In an effort to resolve this issue, an experimental system that integrates Binary Pressure-Sensitive Paint and Stereo Photogrammetry into a single system has been developed. Stereo Photogrammetry utilizes two images of the model to provide quantitative measurements of the displacement and deformation of the model surface. Pressure-Sensitive Paint allows non-intrusive measurements of pressure with high spatial resolution. Binary-Pressure Sensitive Paint uses a reference channel to compensate for errors that result from variations in temperature and illumination over the model surface. An added advantage of binary pressure-sensitive paint is the elimination of all but a single wind-off measurement, thus increasing tunnel productivity. Here we report the results of several experiments that demonstrate the capability of Binary Pressure-Sensitive Paint in low speed wind tunnels. Finally, the integration of pressure and deformation measurements into a single system is demonstrated by experimental measurements of pressure and deformation on an Unmanned Combat Air Vehicle model in the Subsonic Aerodynamics Research Laboratory wind tunnel at Wright-Patterson Air Force Base.

## Introduction

In the continuing effort to shorten the aircraft design cycle the use of numerical tools in the design process has become more common. While these numerical tools can provide quick feedback to the designer, the accuracy of these numerical predictions must be verified. This issue is often addressed by comparing these numerical results with a select set of experimental data. Experimental techniques that produce high-spatial resolution image based data such as Pressure-Sensitive Paint<sup>1</sup> (surface pressures), Planar Doppler Velocimetry<sup>2</sup> (3-component velocity), and Shear and Stress Sensitive Films<sup>3</sup> (shear stress) can aid in the code validation process. Here again the issue of shortening the design cycle has led to the use of rapid manufacturing processes for the construction of the models. To complete the code validation process in the design cycle, the experimental and numerical data must be compared. Here, photogrammetric techniques<sup>4</sup> are utilized to map the image based data onto the 3-D geometry of the numerical model. Thus the numerical and experimental data may be compared on the numerical geometry.

One remaining issue that hinders the comparison of the experimental measurements and numerical predictions is the accuracy and structural integrity of the physical model. The computations are preformed on a perfect model that is infinitely rigid while the physical model

---

\* Member AIAA

includes imperfections and deforms under aerodynamic loading. The use of rapid prototyping techniques often produces a model that is less rigid and thus this model deforms more under aerodynamic loading. Techniques such as Stereo Photogrammetry<sup>5</sup> and Projection Moire Interferometry<sup>6</sup> (PMI) have been demonstrated for experimentally measuring the displacement and deformation of wind tunnel models under aerodynamic loads. In this report we describe a system that combines Pressure Sensitive Paint and Stereo Photogrammetry to acquire simultaneous measurements of pressure and geometry on aerodynamic models. The final result is a system that measures pressure and the surface geometry of the model when the pressure data was acquired. This data should prove valuable for the validation of the numerical predictions and aid in the improvement of the design process.

### Pressure Sensitive Paint

Traditional techniques for acquiring measurements of surface temperature and pressure on wind tunnel models have utilized embedded arrays of thermocouples and pressure taps. This approach requires significant model construction and setup time while producing data with limited spatial resolution. Furthermore, physical constraints such as mechanical movement or section thickness can preclude the use of thermocouples and pressure taps in certain regions of a model. An alternative approach that has received considerable attention over the past 15 years is the use of luminescent probes that are sensitive to temperature and pressure. These techniques, known as Temperature and Pressure-Sensitive Paint<sup>1</sup>, have produced high spatial resolution measurements of temperature and pressure on surfaces that have in the past proven to be inaccessible.

While Pressure-Sensitive Paints (PSP) have demonstrated significant potential in high-speed wind tunnels, several issues that limit the accuracy<sup>7</sup> of the technique have been identified. Among these issues are errors due to model displacement and deformation, instability of the illumination source, photo-degradation and sedimentation of the painted surface, and non-uniform temperatures on the model surface. Errors in PSP measurements have prevented wide deployment of PSP systems for numerous applications. An approach that minimizes the errors in PSP measurements would provide a significant benefit for research.

A typical pressure sensitive paint is composed of two parts, an oxygen-sensitive fluorescent molecule, and an oxygen permeable binder. The pressure sensitive paint method is based on the sensitivity of certain luminescent molecules to the presence of oxygen. When a luminescent molecule absorbs a photon, it transitions to an excited singlet energy state. The molecule then typically recovers to the ground state by the emission of a photon of a longer wavelength. In some materials oxygen can interact with the molecule such that the transition to the ground state is non-radiative, this process is known as oxygen quenching. The rate at which these two processes compete is dependent on the partial pressure of oxygen present, with a higher oxygen pressure quenching the molecule more, thus giving off a lower intensity of light.

Image based pressure measurements using PSP are accomplished by coating the model surface with the paint and illuminating the surface with light of the appropriate wavelength to excite the luminescent molecule. The surface is imaged through a long-pass filter to separate the luminescent signal from the

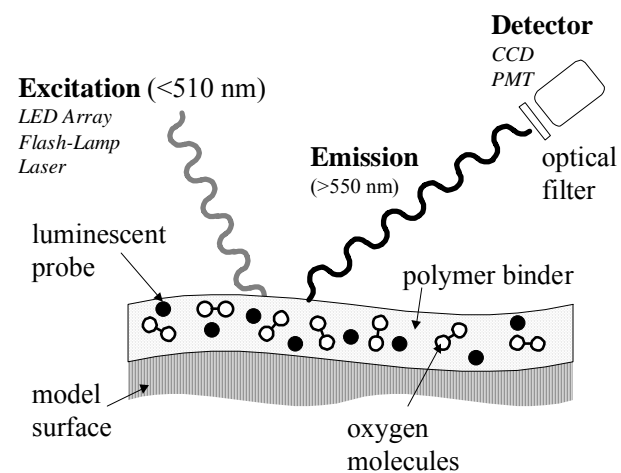


Figure 1 Basic PSP system.

excitation light and the luminescent signal distribution is recorded. A schematic of the system is shown in Figure 1. Unfortunately, the luminescent signal from the paint is not only a function of pressure. The luminescence varies with illumination intensity, probe concentration, paint layer thickness, and detector sensitivity. These spatial variations result in a non-uniform luminescent signal from the painted surface. The spatial variations are eliminated by taking the ratio of the luminescent intensity of the paint at an unknown test condition,  $I$ , with the luminescent intensity of the paint at a known reference condition,  $I_o$ . Using this *wind-on wind-off* ratio, the response of the system can be modeled using a modification of the Stern-Volmer equation.

$$\frac{I_o}{I} = A(T) + B(T) \frac{P}{P_o} \quad (1)$$

### Uncertainty in PSP Measurements

Sources of uncertainty for PSP measurements have been investigated and modeled by Liu<sup>7</sup>. These error sources include temperature, illumination, model displacement/deformation, sedimentation, photo-degradation, and camera shot noise. Liu concluded that the major sources of error were temperature and illumination. These two sources of error will be discussed and the minimization of these errors through the use of binary PSP will be discussed. Errors due to temperature will be considered first.

Note in equation 1 that the Stern-Volmer coefficients,  $A(T)$  and  $B(T)$  are functions of temperature. The Stern-Volmer coefficients are temperature dependent because temperature affects both non-radiative deactivation and oxygen diffusion in a polymer. In fact, the temperature dependence of  $A(T)$  is due to thermal quenching while the temperature dependence of  $B(T)$  is related to the diffusivity of oxygen in a polymer binder. The temperature sensitivity of the Stern-Volmer coefficients are modeled following Liu<sup>7</sup> as:

$$A(T) = A(T_o) \left[ 1 + \frac{E_{nr}}{R T_o} \left( \frac{T - T_o}{T_o} \right) \right] \quad B(T) = B(T_o) \left[ 1 + \frac{E_p}{R T_o} \left( \frac{T - T_o}{T_o} \right) \right] \quad (2)$$

Temperature sensitivity can lead to errors in converting the intensity distributions to pressure. This is demonstrated by considering a calibration of a PSP composed of Platinum tetra(pentafluorophenyl)porphine (PtTFPP) in Fluoro/Isopropyl/Butyl (FIB), shown in Figure 2. The quantity  $I_o/I$  is a monotonic function of pressure along each isotherm. The wind-on and wind-off images however, must be acquired at the same temperature if the conversion to pressure is to be free from temperature errors. A second temperature related issue is the slope of the curve along each isotherm. For most PSP's, the slope of the sensitivity curve is a function of temperature. An accurate measurement of the absolute temperature is necessary to correctly convert the intensity ratio to pressure. An important property of the PtTFPP/FIB paint is the property of ideality<sup>8</sup>. For an ideal paint, the slope of the sensitivity curve is independent of temperature. This property is of significant value for minimizing temperature errors in PSP measurements. It is also a significant advantage in the production of a temperature compensating Binary PSP.

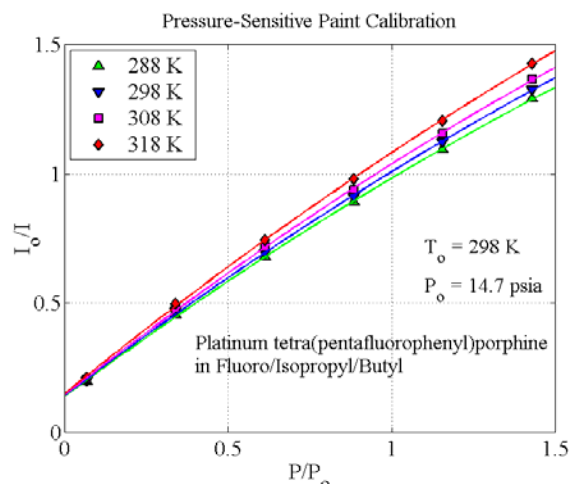


Figure 2 Calibration of PtTFPP/FIB.

For radiometric PSP, errors in pressure measurements due to temperature are largely the result of changes in the temperature of the model surface between the acquisition of the wind-off and wind-on image. However, any temperature gradient on the model surface will still result in a temperature-induced error in the pressure measurements. These temperature gradients can be the result of model construction, tunnel operation, or fluid dynamics. The UCAV model, for example, is constructed using an internal metal structure and a polymer resin. The thermal signature of the internal structure is apparent when the surface of the model is subjected to a heat flux. The model is commonly exposed to a heat flux due to changes in tunnel Mach number. This condition is most apparent during tunnel startup. Even after the model has reached thermal equilibrium the temperature distribution on the model is not necessarily uniform. One example of a temperature gradient generated by the external flow is boundary layer transition. In this case, one must consider the recovery temperature defined as:

$$T_r = T + \frac{V^2}{2 C_p} r \quad (3)$$

In this equation,  $T_r$  is the recovery temperature,  $T$  is the static temperature,  $V$  is the fluid velocity,  $C_p$  is the specific heat of the fluid, and  $r$  is the recovery factor. The recovery factor for a boundary layer with no pressure gradient is a function of Prandtl number and the state of the boundary layer. According to White<sup>9</sup>, this relationship is:

$$r = \sqrt{\text{Pr}} = 0.841 \Rightarrow \text{lam.} \quad r = \sqrt[3]{\text{Pr}} = 0.891 \Rightarrow \text{turb.} \quad (4)$$

Using equation 3 and equation 4 and assuming a Mach number of 0.4, boundary layer transition should result in a temperature gradient of about 0.5 degrees Kelvin. The UCAV model is constructed from a low thermal conductivity material therefore the boundary condition is close to adiabatic. The temperature gradient will be close to the 0.5 Kelvin but the model surface will reach a steady state temperature quickly. Assuming the temperature sensitivity of PTFPP/FIB, this temperature gradient will produce an error in pressure of 0.1 psi.

The relationship between surface illumination and paint luminescence is linear; therefore, any change in surface illumination will result in an equal change in paint luminescence. Errors in pressure measurements caused by variations in surface illumination can stem from several sources. Consider utilizing a point source for the illumination of a surface as shown in Figure 3. The relationship between illumination intensity at a point on the surface and the distance between the source and the point of interest are an inverse function of the distance squared. Any movement of the painted surface or illumination source will result in a change in the distance between these two points, and thus a change in the illumination intensity at the surface. This movement can result from deformation of the model surface, or physical displacement of the model or illumination source. Another source of illumination errors is the temporal stability of the illumination source. Any variation of the intensity of the illumination source between the *wind-off* and *wind-on* images will register as an error in illumination.

### Binary Pressure-Sensitive Paint

One means of dealing with the issue of illumination errors is to employ a reference probe. In fact, several groups have successfully demonstrated this approach<sup>10, 11</sup>. The goal is to use the luminescence of the reference probe to correct for variations in the luminescence of the signal probe (the pressure sensor) that are due to variations in illumination. This is accomplished by taking a ratio of the luminescence of

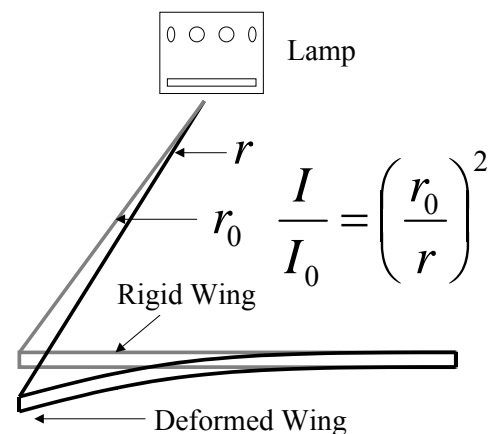


Figure 3 Error due to illumination.

the signal probe to the luminescence of the reference probe. Assuming that both the signal and probes response is linearly proportional to the local illumination and probe number density the resulting function is

$$R(P, T, n_s, n_R) = \frac{F_S(P, T) n_s I}{F_R(P, T) n_R I} \quad (5)$$

The dependence of R on illumination has been removed, however R is still a function of temperature, pressure, and the concentration of each probe. If the distributions of the signal and reference probes are identical, the dependence on probe concentration is removed. This condition however, is difficult to achieve. To eliminate the effects of probe concentration, the standard *wind on* and *wind off* ratio (a ratio of ratios) is applied

$$S(P, T) = \frac{R_0(P_0, T_0) n_s / n_R}{R(P, T) n_s / n_R} = \frac{R_0(P_0, T_0)}{R(P, T)} \quad (6)$$

The system response S is now a function of pressure and temperature only. At first glance, this ratio of ratios procedure may not seem to be an improvement over the standard radiometric approach. However, the relative concentration of each probe is static therefore only a single *wind-off* is needed. This is a significant improvement in tunnel productivity as it reduces the number of *wind-off* conditions by a factor of two.

Selection of the reference probe is by no means trivial. The reference probe must be excited by the same illumination source that is used to excite the signal probe and the luminescence of the reference probe must be spectrally separated from the luminescence of the signal probe. The reference probe must be compatible with the solvents and binders that are used for the signal probe. Finally to maximize the pressure sensitivity of the system, the reference probe should exhibit as little sensitivity to pressure as possible. A paint that meets these criteria is known as a Self-Referencing Paint.

With illumination removed from equation 6 the goal becomes minimizing the sensitivity of the system to temperature. The approach utilized involves allowing the reference probe, which is eliminating sensitivity to illumination, to compensate for the temperature sensitivity as well. This is accomplished by adding two constraints to the selection criteria already outlined for a self-referencing paint. 1) The combination of the signal probe and paint binder must form an ideal paint and 2) the temperature sensitivity of the reference probe must match the temperature sensitivity of the ideal paint. A PSP composed of PtTFPP/FIB is a good candidate for a binary paint. PtTFPP/FIB is an ideal paint with low temperature sensitivity. A binary PSP composed of PtTFPP/FIB and a selected reference probe has been used to produce a PSP with a low temperature sensitivity. The calibration of this paint is shown in Figure 4. The temperature sensitivity of ISSI Binary FIB is less than 0.05% per degree K over a range of temperatures from 5 – 45 C and pressures from 1 – 20 psia.

### Stereo Photogrammetry

The concept of image based measurements of model displacement and deformation is not unique. Image based

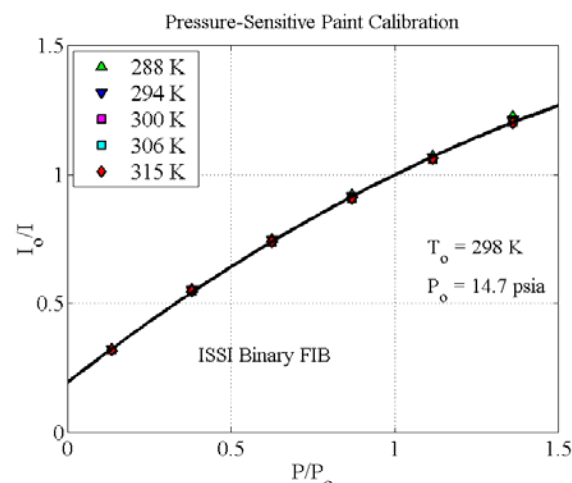


Figure 4 Calibration of ISSI Binary FIB.

measurements in wind tunnels have been used to determine quantities such as model deformation<sup>5,6</sup> and angle of attack<sup>12</sup> using several techniques. Conceptually, the experimental measurements of the model geometry may be used to modify the numerical mesh of the model. This modified mesh could then be utilized for a subsequent numerical prediction. This modified geometry would facilitate a more accurate comparison of the experimental and numerical results since the experimental data was acquired on the deformed model. With this motivation in mind, the goal is to combine measurements of pressure, using PSP, with a simultaneous measurement of the model geometry, using Stereo Photogrammetry.

The basic setup for Stereo Photogrammetry is shown in Figure 5. A series of high contrast markers are placed on a surface and the real world  $(x_w, y_w, z_w)$  coordinates of these markers are known or measured. The surface is then projected onto the image plane of a camera from two perspectives through a pair of cameras and the coordinates  $(x, y)$  of each marker in the image plane is determined. As the surface displaces or deforms the location of the markers on the image plane is modified. Again, the coordinates  $(x', y')$  of each marker in the image plane are determined. The new real world location of each marker  $(x'_w, y'_w, z'_w)$  is then determined using a calibration. Conceptually this process is quite simple, however the process of determining the calibration should be discussed in more detail.

General photogrammetry often requires a complex calibration process. A point at real world location  $(x_w, y_w, z_w)$  is projected onto the image plane of the camera at  $(x, y)$ . If the exact position and orientation of each camera is known, the real world position of the point can be determined from trigonometry relationships. However, precisely measuring the orientation and location of the cameras can be difficult. The method of photogrammetry instead uses a generalized matrix model to form a map from the camera image planes back to the real world coordinate system.

Calibration points are used to provide known locations in real space that correspond to certain known locations in the camera image planes. The cameras must all contain the calibration points within their field of view. For each calibration point with real world position  $(x_w, y_w, z_w)_n$ , each camera sees the point on its image plane at a unique location  $(x, y)_n$ . This transformation can be described by a set of functions:

$$\begin{aligned} (x, y)_n &= f_n(x_w, y_w, z_w, a_1, \dots, a_N) \\ n &= 1, 2, \dots, N \end{aligned} \quad (7)$$

Through the use of calibration points, the coefficients  $a_n$  can be determined. For the purposes of aerodynamic models, the model geometry is well defined and the displacements are small compared to the scale of the model. These conditions allow the creation of a linear system of equations connecting displacements in image plane  $(\Delta x, \Delta y)_n$  with model deformations  $(\Delta x_w, \Delta y_w, \Delta z_w)$  in the calibration points

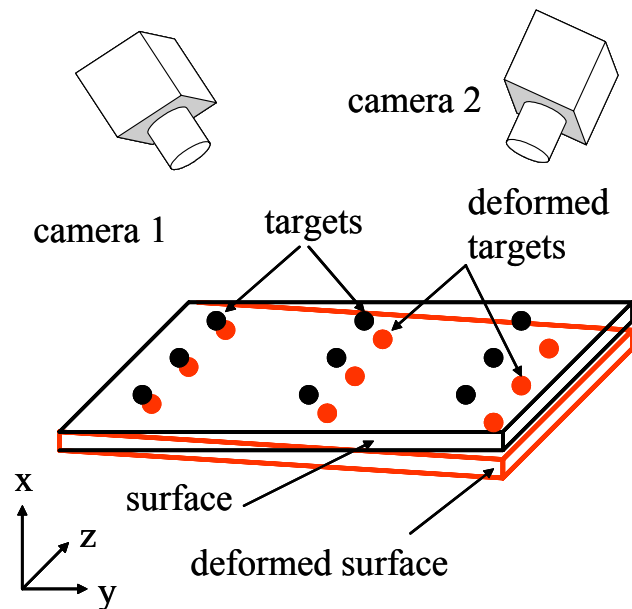


Figure 5 Setup for Stereo Photogrammetry.

$$\begin{aligned}
 (\Delta x, \Delta y)_n &= f_{nX} \Delta x_w + f_{nY} \Delta y_w + f_{nZ} \Delta z_w \\
 n &= 1, 2, \dots, N \\
 f_{nX} &\text{ is partial derivative in } (x_w, y_w, z_w)
 \end{aligned}
 \tag{8}$$

For a data set that uses two cameras, this system is over-determined and the linear system can be solved.

A few summary comments on the Stereo Photogrammetry system are order. Generally aerodynamic models are three dimensional and include features, such as pressure taps and mechanical details, at well defined locations. This yields a calibration image that includes markers with known world coordinates in all three dimensions. In this case the model itself can act as the calibration image thus simplifying the calibration procedure and improving tunnel productivity. Finally, the output of the system is the real world coordinates of the markers on the model. These coordinates provide information on all three components of deformation at each marker, however no intermediate information is supplied. While it possible for these aerodynamic models to include higher order bending and flapping modes it is not a common problem due to the short, stiff components of the model. The final issue is to combine the PSP and Stereo Photogrammetry systems.

Binary PSP requires two images of the model, a signal and reference image. While it is common to acquire these images using a single camera and a filter switch, two independent views of the model are also acceptable. The latter approach is used in developing the combined Binary PSP Stereo Photogrammetry system for this experiment. The basic setup is similar to Figure 5 with one camera acting as the signal camera and the other acting as the reference camera. The signal camera is placed near the nose of the model and the reference camera is placed near the tail providing a stereo view of the model. The system is calibrated by acquiring images of the model at two angles of attack and the location of the pressure taps on the model were measured using a Coordinate Measurement Machine.

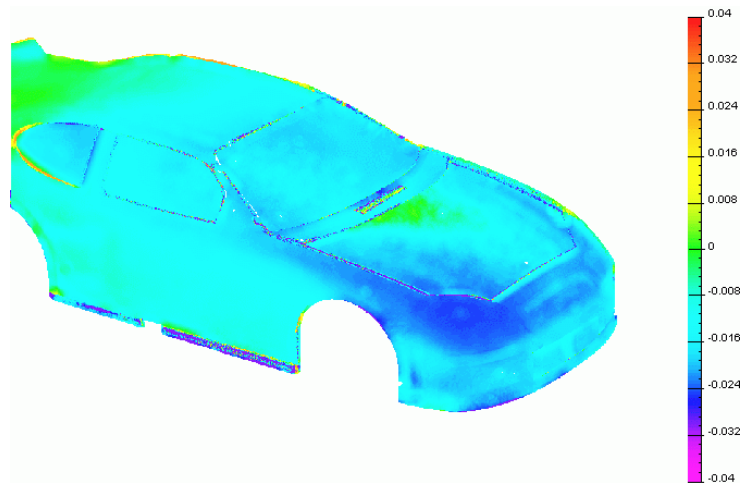


Figure 6 Reference channel at 50 m/s.

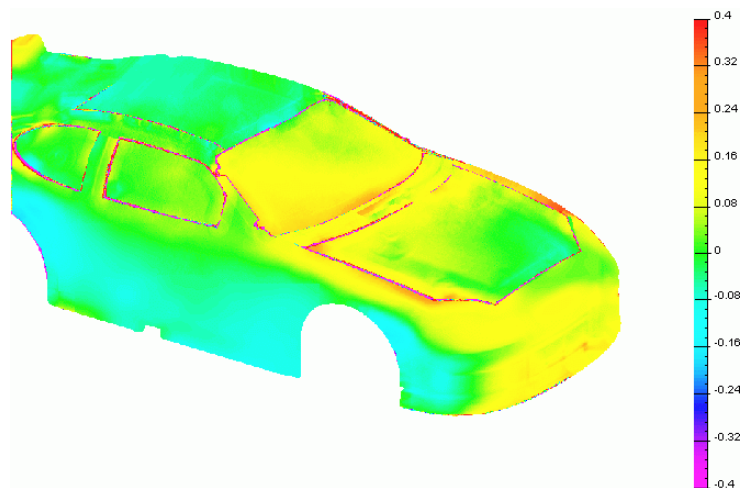


Figure 7 Binary data at 50 m/s.

## Results

Two experimental campaigns will be discussed. The first experiment is an application of Binary PSP in a low speed environment and the second demonstrates the combined Binary PSP and Stereo Photogrammetry systems.

### Pressure on an Automotive Model at Low Speed

Measurements of pressure in low speed tunnels using PSP has been an area of significant interest for several years.

Generally, the effects of temperature and model deformation/displacement have significantly degraded the quality of the data. This is demonstrated in the current experiment. A one twenty-fourth scale car model was painted with BF405 (Binary FIB PSP) and placed in the Air Force Institute of Technology (AFIT) low speed wind tunnel in Dayton Ohio. This is an open circuit wind tunnel with a maximum speed of Mach 0.2 and a 3 ft. by 4 ft. test section. The model was illuminated with four LM2-405 arrays and imaged using a PCO-1600 CCD camera through a FS-3 filter switch. Test were performed at 50 m/s and 20 m/s at approximately 0 and 10 degrees yaw. At 50 m/s the dynamic pressure is approximately 0.2 psi, this would correspond to a change in intensity from the PSP of about 1%. To demonstrate the effects of model movement, the wind-off and wind-on data that was acquired through the reference channel was ratioed and is presented in Figure 6. Note here that the signal from the reference channel, which is not sensitive to pressure, has changed by as much as 3% and varies by over 1% for different regions of the model. These variations in intensity are attributed to movement and deformation of the model at the wind-on condition. Temperature effects are minimized in this experiment since this is an open circuit wind tunnel, they are not however negligible. Consider that the total anticipated signal change due to pressure is about 1%, however the errors due to illumination are larger than this. Next the data was reduced using both the signal and reference images and the resulting pressure distribution is

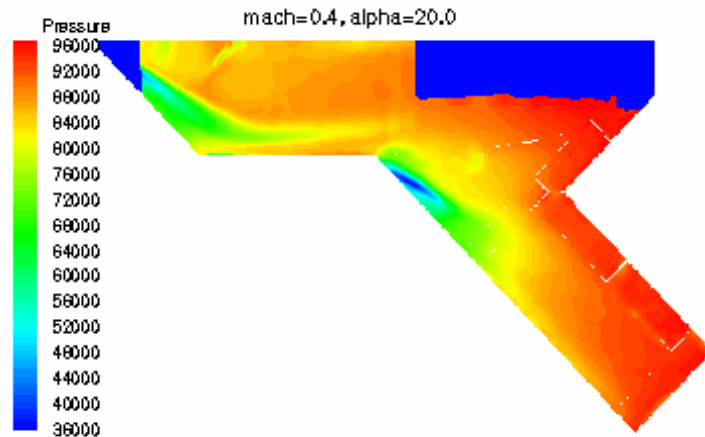


Figure 8 PSP measurements at M 0.4 and  $\alpha=20^\circ$ .

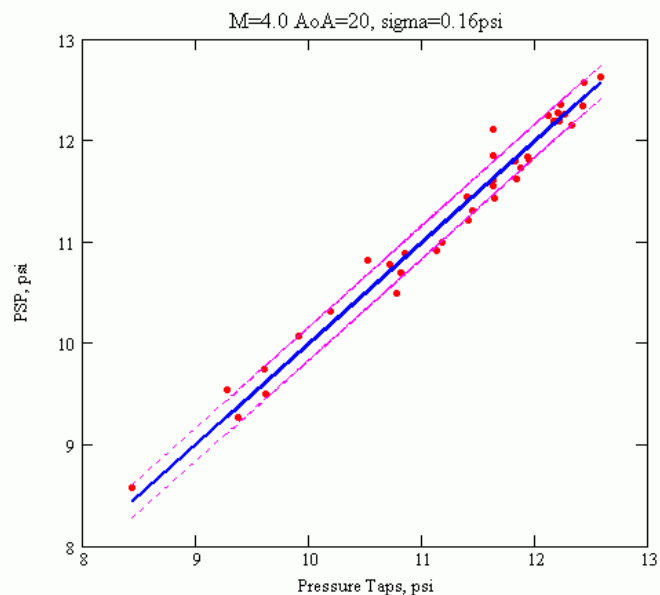


Figure 9 Comparison of PSP and pressure taps.

shown in Figure 7. Note that the maximum pressure is about equal to the tunnel dynamic pressure. Regions of high pressure are evident on the front bumper and the windshield. As the flow accelerates around the front bumper and down the side of the car a region of low pressure is evident. Compensation for model movement is essential for general application of PSP to low speed tests.

### UCAV in the SARL

The UCAV experiments were performed in the Subsonic Aerodynamics Research Laboratory (SARL) wind tunnel at Wright-Patterson Air Force Base. The SARL is an open-circuit wind tunnel with a 3.05 meter by 2.13 meter test section and a maximum Mach number of 0.5. The tunnel provides excellent optical access with Pyrex windows on both the top and each side of the test section.

The Boeing UCAV model is a hybrid design built by John Hopkins University Applied Physics Laboratory. The model is composed of an internal metal structure to withstand the aerodynamic loading and an external geometry constructed using a rapid-prototype stereo-lithography polymer. The model has a lambda wing with a span of approximately 4 feet and length of 3 feet. Control surfaces on the trailing edge were adjusted to  $-20$ ,  $0$ , and  $+20$  degrees for the current tests. Test conditions included angle of attach of 12 and 20 degrees at Mach numbers of 0.2 and 0.4.

The first goal of this experimental campaign was to demonstrate Binary PSP in the SARL. Demonstration of simultaneous PSP and deformation measurements was a secondary goal for this entry. For these reasons, two experimental setups were employed. One specifically for acquiring PSP measurements on the entire UCAV model, and one for demonstrating PSP and deformation measurements on the UCAV wing. For demonstration of Binary PSP measurements the setup included two PixelVision SpectraVideo cameras. The SpectraVideo is a cooled, back-illuminated CCD with a full-well capacity of 300,000 photo-electrons and a 16-bit readout. One camera viewed the front half of the model while the second camera viewed the back half. Each camera was combined with a 50mm f/4 Nikon lens and a FS-2 filter switch. The filter switch holds up to four, 2 inch filters in front of the camera lens. The filter switch communicates with the data acquisition program through an RS-485 interface. The camera and filter switch are mounted onto an optical rail to form a single unit. Paint illumination is provided by four LM4-405 arrays.

One source of noise for PSP measurements that has been an issue in past SARL tests is background noise. The SARL is an open circuit tunnel and therefore, it is difficult to eliminate ambient light. In general, some level of background lighting is always present for PSP tests. This issue is usually resolved by acquiring an image of the test article with the illumination off. This background is then subtracted from the data images to remove the background noise. This procedure assumes that the background lighting is constant, this is not the case in the SARL. The background varies from about 1% of the dynamic range of the camera to over 30% of the dynamic range of the camera due to the

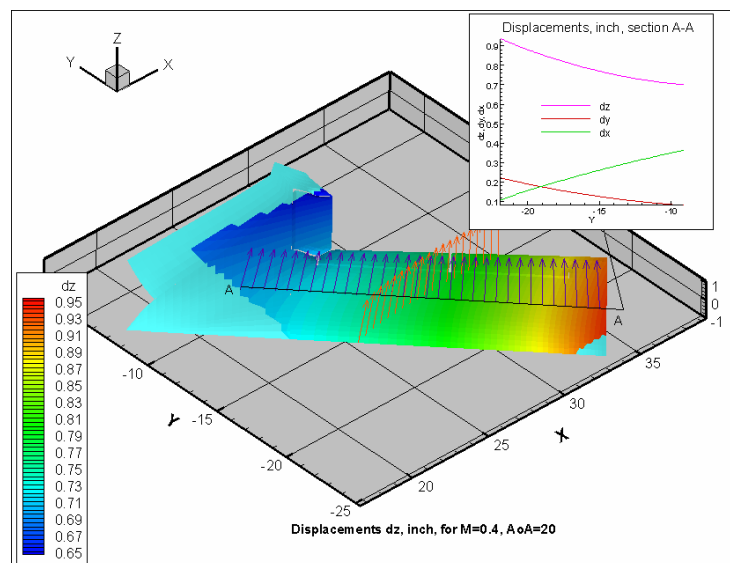


Figure 10 Deformation and deflection of the model.

position of the sun. Furthermore, this background can change substantially in a short time due to cloud cover or other shadows. To minimize this dynamic background effect, a background image was acquired on every fifth exposure. These wind-on backgrounds are then used to minimize the error due to background lighting.

The pressure coefficient for the UCAV model at Mach 0.4 and 20 degrees angle of attach is shown in Figure 8. This distribution was obtained using the Binary PSP. The defining aerodynamic features are evident in this image. The strong vortex off of the nose of the model weakens and propagates along the side of the model. Near the wing/body junction, a secondary vortex appears on the wing and sweeps outboard along the wing. After a short distance, this vortex bursts and continues to move along the span of the wing.

An estimate of the accuracy of the PSP measurements is obtained by plotting the pressure from the PSP near the taps versus the tap pressure. This data was compiled at over 40 tap locations and is shown in Figure 9. The mean squared deviation in this plot is about 0.1 psi. This deviation is substantially larger than would be expected. In this case, the major source of error is believed to be background illumination. Again, the SARL is an open circuit tunnel and therefore, it is difficult to eliminate ambient light. For this test, only four 4-inch LED lamps were available. This level of illumination required longer exposure times and therefore, higher levels of background noise. A further complication was the variation of the background previously discussed. In an effort to minimize this dynamic background effect, a background image was acquired on every fifth exposure. While these interlaced improved the signal to noise, some error remains. To minimize this problem on future tests, more lamps are required and background and data shots should be alternated to improve signal to noise.

The demonstration of simultaneous PSP and deformation measurements employed the same data acquisition system. In this case however, the view of each camera was repositioned to include the wing of the UCAV model. In this case, the calibration process included setting the model to angles of attach of 12 degrees and 20 degrees. Images of the wing were acquired at these conditions and the positions of the pressure taps at each angle of attack were measured. The pressure taps served as markers for both the PSP resection process and for the Stereo Photogrammetry measurements. Data acquisition again included a set of wind-off and wind-on images through each filter. This data was processed to determine pressure in a manner identical to the preceding discussion. To determine model deflection and deformation, the position of the pressure taps on the bitmaps were determined and converted to world coordinates using the calibration. This data set represents a discrete set of information. These data points were used as the basis of an interpolation procedure to produce a continuous map of wing deflection.

The deformation of the model at 20 degrees angle of attach and Mach 0.4 is shown in Figure 10. These measurements indicate both a bulk shift of the model and bending of the wing. The bulk shift is approximately 0.6 inches at the spine of the model near the wing/body junction. The bending of the wing from the body to the tip is about 0.4 inches for this test condition. The bulk shift of the model can be a significant source of error for standard PSP. The wing bending of 0.4 inches is close to the value predicted for this model prior to the test. It is noted that the pseudo-continuous results presented here are the result

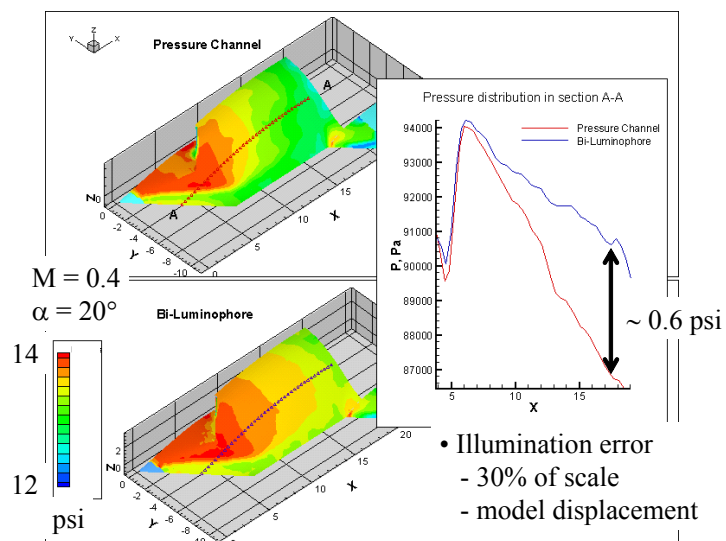


Figure 11 Comparison of Single and Binary Data.

The bulk shift of the model can be a significant source of error for standard PSP. The wing bending of 0.4 inches is close to the value predicted for this model prior to the test. It is noted that the pseudo-continuous results presented here are the result

of deformation measurements at a series of discrete points on the model. The data from these discrete points was interpolated to generate the continuous distribution shown here.

As was the case for the car model, the bulk shift of the model and deformation is a significant source of error for standard PSP as shown in Figure 11. Here we compare the Binary data to the pressure distribution that is obtained by simply reducing the pressure channel data. Neglecting the effects of the 0.6 inch displacement produces an error of over 0.5 psi on the body of the model. This is approximately 30% of the total pressure range for this model. Again, the utility of the reference channel in compensating for model movement is demonstrated.

## Conclusions

A system capable of simultaneous pressure and deformation measurements has been developed. This system integrates Binary Pressure-Sensitive Paint and Stereo Photogrammetry into a single system. Binary Pressure-Sensitive Paint provides PSP measurements that are compensated for errors from temperature and illumination. Stereo Photogrammetry utilizes two images of the model to provide quantitative measurements of the displacement and deformation of the model surface. Experimental measurements of pressure and deformation using the integrated system have been conducted on a UCAV model in the SARL wind tunnel at Wright-Patterson Air Force Base. The mean squared deviation between the Pressure-Sensitive Paint results and the pressure taps was  $\sim 0.1$  psi. Deformation measurements indicate a bulk displacement of the model as well as bending of the wing under aerodynamic load.

- 
- <sup>1</sup> T. Liu, Campbell, B., Burns, S. Sullivan, J., "Temperature and Pressure-Sensitive Paints in Aerodynamics", *Applied Mechanics Reviews*, Vol. 50, n 4, pp. 227-246
  - <sup>2</sup> G. Elliott, J. Crafton, H. Baust, C. Tyler, C. Carter, T. Beutner, "Evaluation and Optimization of a Multi-component Planar Doppler Velocimetry System", AIAA-2005-0035
  - <sup>3</sup> S. Fonov, L. Goss, G. Jones, J. Crafton, V. Fonov, "New Method for Surface Pressure Measurements", AIAA-2005-1029
  - <sup>4</sup> Bell, J.H., McLachlan, B.G., "Image Registration for Pressure-Sensitive Paint Applications", *Experiments in Fluids*, Vol. 22, n 1, pp. 78-86
  - <sup>5</sup> Schairer, E. T., Hand, L. A., "Measurements of Unsteady Aeroelastic Model Deformation by Stereo Photogrammetry" *Journal of Aircraft*, Vol. 36, n 6, pp 1033-1040
  - <sup>6</sup> Fleming, G.A., Gorton, S.A., "Measurements of rotorcraft blade deformation using Projection Moire Interferometry", *Journal of Shock and Vibration*, Vol. 7, n 3
  - <sup>7</sup> Liu, T., Guille, M., Sullivan, J. P., "Accuracy of Pressure Sensitive Paint", *AIAA Journal*, Vol. 39, n 1
  - <sup>8</sup> Puklin, E., Carlson, B., Gouin, S., Costin, C., Green, E., Ponomarev, S., Tanji, H., Gouterman, M., "Ideality of Pressure-Sensitive Paint. I. Platinum Tetra(pentafluorophenyl)porphine in Fluoroacrylic Polymer", *Journal of Applied Polymer Science*, Vol. 77, pp. 2795-2804
  - <sup>9</sup> White, F. M., "Viscous Fluid Flow", 2<sup>nd</sup> ed., McGraw-Hill, 1991
  - <sup>10</sup> Bykov A, Fonov S, Mosharov V, Orlov A, Pesetsky V, Radchenko V. Study Result for the Application of Two-component PSP Technology to Aerodynamic Experiment. *AGARD'97*
  - <sup>11</sup> Khalil G, Costin C, Crafton J, Jones E, Grenoble S, Gouterman M, Callis J, Dalton L. Dual Luminophor Pressure Sensitive Paint I: Ratio of Reference to Sensor Giving a Small Temperature Dependence. *Sensors and Actuators B*, Vol. 97, n 1 , pp. 13-21
  - <sup>12</sup> Burner, A. W., Liu, T., "Videogrammetric Model Deformation Measurement Technique", *Journal of Aircraft*, Vol. 38, n 4, pp. 745-754